

AperTO - Archivio Istituzionale Open Access dell'Università di Torino

Combined untargeted and targeted fingerprinting with comprehensive two-dimensional chromatography for volatiles and ripening indicators in olive oil

This is the author's manuscript

Original Citation:

Availability:

This version is available <http://hdl.handle.net/2318/1589438> since 2016-12-01T15:37:20Z

Published version:

DOI:10.1016/j.aca.2016.07.005

Terms of use:

Open Access

Anyone can freely access the full text of works made available as "Open Access". Works made available under a Creative Commons license can be used according to the terms and conditions of said license. Use of all other works requires consent of the right holder (author or publisher) if not exempted from copyright protection by the applicable law.

(Article begins on next page)

This Accepted Author Manuscript (AAM) is copyrighted and published by Elsevier. It is posted here by agreement between Elsevier and the University of Turin. Changes resulting from the publishing process - such as editing, corrections, structural formatting, and other quality control mechanisms - may not be reflected in this version of the text. The definitive version of the text was subsequently published in *ANALYTICA CHIMICA ACTA*, 936, 2016, 10.1016/j.aca.2016.07.005.

You may download, copy and otherwise use the AAM for non-commercial purposes provided that your license is limited by the following restrictions:

- (1) You may use this AAM for non-commercial purposes only under the terms of the CC-BY-NC-ND license.
- (2) The integrity of the work and identification of the author, copyright owner, and publisher must be preserved in any copy.
- (3) You must attribute this AAM in the following format: Creative Commons BY-NC-ND license (<http://creativecommons.org/licenses/by-nc-nd/4.0/deed.en>), 10.1016/j.aca.2016.07.005

The publisher's version is available at:

<http://linkinghub.elsevier.com/retrieve/pii/S0003267016308261>

When citing, please refer to the published version.

Link to this full text:

<http://hdl.handle.net/2318/1589438>

1 **Combined Untargeted and Targeted fingerprinting with comprehensive**
2 **two-dimensional chromatography for volatiles and ripening indicators in**
3 **olive oil**

4
5
6
7
8
9
10 6 Federico Magagna^{1§}, Lucia Valverde-Som^{2§}, Cristina Ruíz-Samblás², Luis Cuadros-Rodríguez²,
11 7 Stephen E. Reichenbach³, Carlo Bicchi¹, Chiara Cordero^{1*}

12
13
14
15
16 9 ¹ Dipartimento di Scienza e Tecnologia del Farmaco, Università di Torino, Turin, Italy

17 10 ² Department Analytical Chemistry, Faculty of Science, University of Granada, C/Fuentenueva
18 11 s/n, 18071, Granada, Spain

19 12 ³ University of Nebraska – Lincoln, Lincoln NE 68588-0115, USA

20
21
22
23
24
25 15 § Federico Magagna and Lucia Valverde-Som, listed in alphabetical order, equally contributed
26 16 to this work

27
28
29
30 19 * Address for correspondence:

31 20 Prof. Dr. Chiara Cordero - Dipartimento di Scienza e Tecnologia del Farmaco, Università di

32 21 Torino, Via Pietro Giuria 9, I-10125 Torino, Italy – e-mail: chiara.cordero@unito.it;

33 22 Phone: +39 011 6707662; Fax: +39 011 2367662

25 **Abstract**

1
2
3
4
5
6
7
8
9
10
11
12
13
14
15
16
17
18
19
20
21
22
23
24
25
26
27
28
29
30
31
32
33
34
35
36
37
38
39
40
41
42
43
44
45
46
47
48
49
50
51
52
53
54
55
56
57
58
59
60
61
62
63
64
65

26 Comprehensive two-dimensional gas chromatography (GC×GC) is the most effective
27 multidimensional separation technique for in-depth investigations of complex samples of
28 volatiles (VOC) in food. However, each analytical run produces dense, multi-dimensional data,
29 so elaboration and interpretation of chemical information is challenging.

30 This study exploits recent advances of GC×GC-MS chromatographic fingerprinting to study
31 VOCs distributions from Extra Virgin Olive Oil (EVOO) samples of a single botanical origin
32 (Picual), cultivated in well-defined plots in Granada (Spain), and harvested at different
33 maturation stages. A new integrated work-flow, fully supported by dedicated and automated
34 software tools, combines *untargeted* and *targeted (UT)* approaches based on peak-region
35 features to achieve the most inclusive fingerprinting.

36 Combined results from untargeted and targeted methods are consistent, reliable, and
37 informative on discriminant features (analytes) correlated with optimal ripening of olive fruits
38 and sensory quality of EVOOs. The great flexibility of the *UT fingerprinting* here adopted
39 enables retrospective analysis with great confidence and provides data to validate the
40 transferability of ripening indicators ((*Z*)-3-hexenal, (*Z*)-2-hexenal, (*E*)-2-pentenal, nonanal, 6-
41 methyl-5-hepten-2-one, octane) to external samples sets. Direct image comparison, based on
42 *visual* features, also is investigated for quick and effective pair-wise investigations. Its
43 implementation with reliable metadata generated by *UT fingerprinting* confirms the maturity
44 of 2D data elaboration tools and makes advanced image processing a real perspective.

45
46
47
48 **Key-words:**

49 Comprehensive two-dimensional gas chromatography-mass spectrometry; untargeted and
50 targeted fingerprinting ; extra virgin olive oil; olives ripening; retrospective investigations

53 1. Introduction

54 Comprehensive two-dimensional gas chromatography (GC×GC) is the most effective
55 multidimensional separation technique for in-depth investigations of complex samples of
56 volatiles in food [1]. The combination, in a single analytical platform, of two separation
57 dimensions with mass spectrometric detection and, when possible, automated sample
58 preparation, delivers highly efficient sample profiling (detailed analysis of single molecular
59 entities) and fingerprinting (rapid, high-throughput screening of samples for distinctive
60 analytical signatures) [2].

61 Each analytical run produces dense, multi-dimensional data, so elaboration and interpretation
62 of chemical information is a challenging task. In addition, food samples generally have a high-
63 degree of chemical multidimensionality [3] thus creating highly complex analytical challenges.
64 In this context, data elaboration strategies should implement smart and productive processes,
65 preferably with a high degree of automation, to make cross-samples analysis efficient and
66 informative.

67 Within the existing methodologies for GC×GC data elaboration [4,5], the approach based on
68 *peak-region* features has been very effective because of its comprehensive and uniform
69 treatment of information from each sample constituent, both knowns and unknowns. Each
70 single chemical entity is characterized by its chromatographic and spectrometric parameters
71 (retention time in both dimensions, detector response, and mass spectral information) and by
72 its absolute and relative position within the pattern of all detectable constituents. As a
73 consequence, the 2D peak-retention pattern of a sample is a diagnostic fingerprint,
74 informative of its composition; and pattern recognition approaches can be successfully applied
75 to improve effectiveness and productivity in multi-sample data elaboration.

76 Although these concepts are not new for the GC×GC community [6], the full automation of
77 these procedures and their implementation in commercial software packages has been
78 achieved only recently. This has limited both routine adoption of the technique for food
79 analysis and investigative strategies for profiling [2,7].

80 Analysis of olive oil volatiles is a challenging and important problem and GC×GC can yield
81 deeper knowledge of the composition of this fraction offering new perspectives for quality and
82 authenticity assessment [8].

83 In spite of the great potential of GC×GC, few studies are available in this field. Vaz Freire et al.
84 [9] first proposed an image-features approach, or more generally a pattern recognition
85 methodology, to investigate the characteristic distribution of volatiles from oils. They adopted
86 open-source image analysis software (Image J, National Institutes of Health) to extract
87 information from small 2D regions located over the separation space and, by Principal

1
2
3
4
5
6
7
8
9
10
11
12
13
14
15
16
17
18
19
20
21
22
23
24
25
26
27
28
29
30
31
32
33
34
35
36
37
38
39
40
41
42
43
44
45
46
47
48
49
50
51
52
53
54
55
56
57
58
59
60
61
62
63
64
65

88 Component Analysis (PCA), selected those regions with the highest discrimination potential.
89 Then, they used targeted profiling to locate known analytes within informative 2D regions.
90 In 2010, Cajka and co-workers [10] exploited the targeted profiling potential of GC×GC-ToF-MS
91 and identified 44 analytes able to discriminate samples of different geographical origin and
92 production year. More recently, Purcaro et al. [8] combined targeted and untargeted analysis
93 with the goal of a chemical blueprint of olive oil aroma defects. This inter-laboratory study
94 confirmed the reliability of GC×GC for detailed profiling of olive oil volatile fractions and
95 introduced an iterative strategy [11,12] to locate sensory-relevant analytes efficiently.

96 This study exploits the most recent advances of GC×GC-MS chromatographic
97 fingerprinting to study VOC distributions from Extra Virgin Olive Oil (EVOO) samples of a single
98 botanical origin (Picual), cultivated in well-defined plots in a single region (Granada, Spain), and
99 harvested at different maturation stages. The principal interest in this application is the quality
100 characteristics related to optimal ripening of olive fruits [13,14]15,16,17,18,19,20,21] and, as a
101 consequence, olive oil classification and perceivable sensory quality [22,23]. In particular, this
102 study proposes an integrated work-flow, fully supported by dedicated software tools, that
103 performs cross-samples comparisons by contemporarily considering characteristic
104 distributions (i.e., sample fingerprints) of both known and unknown compounds. This work-
105 flow integrates both *untargeted* and *targeted (UT) fingerprinting* to realize the most
106 comprehensive results, and so is termed *UT fingerprinting*. Challenges of retrospective analysis
107 and immediacy of image fingerprinting also are discussed because of the advantages they offer
108 in specific investigations.

110 2. Materials and methods

111 2.1. Reference compounds and solvents

112 Pure reference standards of α -thujone, used as Internal Standard (ISTD), at a concentration of
113 100 mg/L in dibutyl phthalate, and *n*-alkanes (n-C9 to n-C25), used for linear retention index
114 (I_s^T) determination, at a concentration of 100 mg/L in cyclohexane, were supplied by Sigma-
115 Aldrich (Milan, Italy).
116 Solvents for *n*-alkanes dilution (toluene and cyclohexane HPLC-grade) and dibutyl phthalate
117 also were from Sigma-Aldrich.

119 2.2. Olive oil samples

120 Olive oil samples of *Picual* variety, harvested in 2014, were supplied by "GDR Altiplano de
121 Granada" (Spain) and were obtained from olives harvested in three different plots in Granada:
122 "812 *Caniles*" (organic production and drip irrigation); "233-234 *Baza*" (conventional
123 production and drip irrigation); and "701 *Benamaurel*" (conventional production and drip
124 irrigation).

125 Each sample was available in duplicate and obtained by mixing olives from at least five
126 different trees in the same plot to have homogeneous and representative samples. Olives
127 were harvested at four different ripening stages: November 10-12, 2014; November 24-28,
128 2014; December 16-17, 2014; and January 12-15, 2015.

129 Samples were analyzed by an accredited laboratory to define quality parameters: acidity (%),
130 peroxide index (mEq O₂/kg), and UV absorption. Samples also were submitted to sensory
131 evaluation by a recognized/official panel [24]. Sample descriptions and acronyms are reported
132 in **Table 1**, together with quality assessments.

134 2.3. Head-space Solid Phase Micro Extraction sampling devices and conditions

135 Volatiles were sampled from the headspace (HS) by HS Solid Phase Micro Extraction (HS-
136 SPME). The sampling protocol was optimized in a previous study [8] and employs a
137 divinylbenzene/carboxen/polydimethylsiloxane (DVB/CAR/PDMS) 50/30 μ m, 2 cm length
138 stableflex fiber from Supelco (Bellefonte, PA, USA).

139 The ISTD (α -thujone) was pre-loaded onto the fiber before sampling through the standard-in-
140 fiber procedure. An ISTD solution, 2.0 μ L, was placed into a 20 mL glass vial and submitted to
141 HS-SPME at 50°C for 15 minutes (min). The fiber then was exposed to the head-space of olive
142 oil samples (1.500 g exactly weighted) in 20 mL glass vials, at 50°C for 40 minutes. Last, the
143 sampled analytes were recovered by introducing the fiber into the S/SL injection port of the

144 GC×GC system at 260°C and thermally desorbed for 5 minutes. Each sample was analyzed in
145 duplicate.

146 **2.4. Comprehensive two-dimensional gas chromatographic system (GC×GC-MS) set-up and** 147 **analysis conditions**

148 GC×GC analyses were performed on an Agilent 6890 unit coupled to an Agilent 5975C MS
149 detector (Agilent, Little Falls, DE, USA) operating in EI mode at 70eV. The GC transfer line was
150 set at 270°C and the MS scan range was 40-240 m/z with a scanning rate of 12,500 amu/s to
151 obtain a spectra generation frequency of 30 Hz.

152 The system was equipped with a two-stage KT 2004 loop-type thermal modulator (Zoex
153 Corporation, Houston, TX) cooled with liquid nitrogen and with the hot jet pulse time set at
154 250 ms with a modulation time of 4 s for all experiments. Fused silica capillary loop dimensions
155 were 1.0 m long and 0.1 mm inner diameter. The column set was configured as follows: ¹D
156 SolGel-Wax column (100% polyethylene glycol)(30 m × 0.25 mm d_c , 0.25 μm d_f) from SGE
157 Analytical Science (Ringwood, Australia) coupled with a ²D OV1701 column (86%
158 polydimethylsiloxane, 7% phenyl, 7% cyanopropyl) (1 m × 0.1 mm d_c , 0.10 μm d_f) from Mega
159 (Legnano, Milan, Italy).

160 Fiber thermal desorption into the GC injector port was under the following conditions:
161 split/splitless injector in split mode, split ratio 1:20, injector temperature 250°C. Carrier gas
162 was helium at a constant flow of 1.8 mL/min. The temperature program was: from 40°C (1
163 min) to 200°C at 3°C/min and to 250°C at 10°C/min (5 min).

164 The *n*-alkanes liquid sample solution for I^T_s determination was analyzed under the following
165 conditions: split/splitless injector in split mode, split ratio 1:50, injector temperature 280°C,
166 injection volume 1 μL .

167

168 **2.5. Raw data acquisition and GC×GC data handling**

169 Data were acquired by Agilent MSD ChemStation ver E.02.01.00 and processed using GC Image
170 GC×GC Software version 2.5 (GC Image, LLC Lincoln NE, USA). Statistical analysis was
171 performed by XLstat (Addinsoft, New York, NY USA) and the PLS Toolbox (Eigenvector Research
172 Inc., West Eaglerock Drive, Wenatchee, WA, USA) for Matlab[®] software (The Mathworks Inc.,
173 Natick, MA, USA).

174

175 **2.6 Profiling and advanced fingerprinting work-flow**

176 The bi-dimensional chromatographic data elaboration proposed here was organized in a
177 sequential work-flow illustrated in **Figure 1**.

178

179 **Insert here Figure 1**

180

181 Untargeted and targeted analyses were performed by applying the *template matching*
182 fingerprinting strategy, introduced by Reichenbach et al. in 2009 [6]. It uses the patterns of 2D
183 peaks' metadata (retention times, MS fragmentation patterns, and detector responses) to
184 establish reliable correspondences between the same chemical entities across multiple
185 chromatograms. The output of template matching fingerprinting is a data matrix of aligned 2D
186 peaks and/or peak-regions, together with their related metadata (¹D and ²D retention times,
187 compound names for target analytes, fragmentation pattern, single ions or total ions
188 response), that can be used for comparative purposes.

189 Targeted analysis (Step 1 of **Figure 1**) focused on about 120 selected compounds, each reliably
190 identified by matching their EI-MS fragmentation pattern (NIST MS Search algorithm, ver 2.0,
191 National Institute of Standards and Technology, Gaithersburg, MD, USA, with Direct Matching
192 threshold 900 and Reverse Matching threshold 950) with those collected in commercial
193 (NIST2014 and Wiley 7n) and in-house databases. As a further parameter to support reliable
194 identification, Linear Retention Indices (I_s^T) were considered and experimental values
195 compared with tabulated ones.

196 Untargeted analysis (Step 2 of **Figure 1**) was based on a *peak-regions* features approach [5]
197 and was performed automatically by GC Image Investigator™ R2.5 (GC-Image LLC, Lincoln NE,
198 USA). The untargeted analysis included all *peak-regions* above the arbitrarily fixed peak
199 response threshold of 5,000 counts together with target peaks from Step 1. This approach
200 [25,26,27,28], briefly described in *Section 3.2*, re-aligned the 48 chromatograms using a set of
201 *registration peaks*. The resulting data matrix was a 48 × 600 (samples × reliable *peak-regions*).
202 Response data from aligned 2D *peak-regions* were used for PCA and results cross-compared to
203 those obtained from target peaks distributions. (See *Section 3.2* for the discussion of results.)

204 *Visual* features fingerprinting, performed as pair-wise image comparison, was the last step of
205 the study (Step 4 of **Figure 1**) and was rendered with “colorized fuzzy ratio” mode [cite
206 Hollingsworth et al., JoCA 1105:51, 2006]. The algorithm computes the difference at each data
207 point between pairs of TICs; a data point is the output of the detector at a point in time. These
208 differences are mapped into Hue-Intensity-Saturation (HIS) color space to create an image for
209 visualizing the relative differences between image pairs in the retention-times plane [29]. A
210 detailed description is provided in *Section 3.4*.

211 3. Results and discussion

1 212 The goal of this study was to evaluate the potential of combining Untargeted and
2 213 Targeted 2D data elaboration approaches based on untargeted *peak-region* features, target
3 214 peaks, and *visual* features to approach to the most inclusive fingerprinting within EVOO
4 215 volatiles: the UT fingerprinting strategy. Based on a sampling design focused on a single
5 216 botanical variety and well-defined geographical locations, VOCs fingerprints were interpreted
6 217 as a function of ripening stage and oil quality.

7 218 This strategy was inspired by a previous study focused on olive oil aroma defects [8], in which
8 219 results clearly indicated that the informative potential of GC×GC-MS to delineate specific
9 220 fingerprints for sensory quality classification of oils. These results showed that a “*strictly*
10 221 *structured experimental design (considering more variables, such as cultivar, geographical*
11 222 *origin, etc.)*” would be mandatory to “*robustly and reliably characterize specific markers and*
12 223 *related characteristics concentration windows*” to support, or even replace, sensory evaluation
13 224 [8]. In addition, it was clear that larger numbers of “external variables” affecting VOCs pattern
14 225 reduce the effectiveness of untargeted approaches.

15 226 In the present study, with fewer sample-set variables, and a data elaboration process that
16 227 combines untargeted and targeted approaches (i.e., *peak-region features, peaks, and visual*
17 228 *features* methods), we achieve highly effective fingerprinting. The proposed work-flow is
18 229 comprehensive yet efficient and fully supported by new commercial software. In addition, we
19 230 validate both the data elaboration strategy and the informative role of some targets by a
20 231 retrospective investigation on VOCs patterns from EVOO, VOO, and *lampante* oils (LOO)
21 232 analyzed in previous studies.

22 233 Following this scheme, we first present and discuss results from targeted analysis, focusing on
23 234 peaks for known informative chemicals and selected VOCs strictly related to the olives’
24 235 geographical location, ripening stage, and product (oils) quality (presence/absence of sensory
25 236 defects). Next, untargeted analysis based on peak-regions features, implemented in the
26 237 second step, is discussed from the perspective of: (a) confirming sample classification results;
27 238 (b) indicating new potential targets; (c) defining chemical indexes of ripening and quality
28 239 through the ratio between informative analytes; and (d) validating the role of informative
29 240 ratios through retrospective elaboration of samples analyzed in previous studies by adopting
30 241 the *UT* template created on the current sample set. The last part of the study aims at
31 242 determining if classification based on peak-regions features could be replaced by direct image
32 243 comparison without losing information about the chemical composition of this fraction. The
33 244 following paragraphs illustrate the research steps and critically discuss results.

34 245

246 3.1 Targeted analysis and samples discrimination

1 247 The sample set is reported in **Table 1** with their quality parameters, sensory evaluation
2 248 results, and commercial classification. Quality metrics (acidity %, peroxide index, UV
3 249 absorbance, and organoleptic assessment) indicated that 6 of the 24 samples were not
4 250 compliant with *Extra-Virgin* classification [30]. These samples, classified as *Virgin* (VOO) and
5 251 *Lampante* (LOO), were from the late ripening stages of the *Baza* and *Benamaurel* plots. This
6 252 quality classification was confirmed by replicate sampling (i.e., *Baz_3_1/_2* and *Baz_4_1/_2*;
7 253 *Ben_4_1/_2*) and was related to sensory defects revealed by the panel (Median of defects - Md
8 254 >0.00). In addition, low-quality samples were connoted by a higher peroxide index and acidity
9 255 %.

10 256 From the available literature [31,32,33,34,35,36,37,38,39], analytes detected in the GC×GC
11 257 data were identified by their EI-MS fragmentation pattern and Linear Retention Indices (I_s^T)
12 258 (see section 2.6 for details). Following the work-flow in **Figure 1**, *template-matching*
13 259 fingerprinting (see Paragraph 2.6) with 119 target peaks was used to map these informative
14 260 chemicals across samples.

15 261 **Figures 2A-B** shows the pseudocolored GC×GC chromatogram of an EVOO sample from the
16 262 *Benamaurel* plot harvested at stage 4 (in January 2015). **Figure 2B** locates the 119 known
17 263 target peaks (empty light green circles) linked to the ISTD (α -tujone black circle) by red lines.

18 264

19 265 **Place here Figures 2A-E**

20 266

21 267 The quali-quantitative distribution of VOCs changed with the harvest stages. The number of
22 268 detectable peaks above a Volume threshold of 4,000 (arbitrarily fixed on the Total Ion Current
23 269 signal) was about 270-280 at the first stage and reached about 360 at the final stage (data not
24 270 shown).

25 271 The effectiveness of GC×GC, in both peak-capacity and overall chromatographic resolution,
26 272 plays a critical role in isolating the information for compounds with similar retention times in
27 273 the ¹D dimension. A zoomed region, highlighted in **Fig 2C**, emphasizes the retention area of
28 274 highly volatile compounds in which some branched hydrocarbons (eluting later in the ²D) are
29 275 separated along the ²D from saturated and unsaturated and carbonyl compounds (e.g.,
30 276 pentanal, hexanal, (*E*)-2-butenal), and 1-penten-3-one, an odor-active volatile deriving from
31 277 linolenic acid degradation), and alcohols (e.g., 1-propanol, 2-butanol, and 2-methyl-2-
32 278 propanol).

33 279 The relative distribution (Normalized 2D Peak Volumes) of the 119 peaks is illustrated as heat-
34 280 map in **Supplementary Figure 1 (SF1)**. Columns are ordered left-to-right by ¹D retention indices

281 (polar phase column, 100% polyethylene glycol). The logarithmic colour map is based on 2D-
282 Peak Volumes divided by ISTD response and is normalized by dividing single values by row
283 standard deviations.

284 **Table 2** reports the 119 target compounds together with their ¹D and ²D retention times, I^T_s ,
285 sensory descriptors, and correlation with oil defects as reported in reference literature
286 [31,32,33,34,35,36,37,38,39]. 2D Peak Normalized Volumes (average values of two analytical
287 replicates) are provided as Supplementary information (**Supplementary Table 1- ST1**).

288 The target analytes distribution (Normalized 2D volumes) was adopted as an informative
289 fingerprint for possible discrimination of samples within different harvest stages and, in
290 particular, to locate and validate specific indicators of ripeness, and, when feasible, odor-active
291 compounds related to sensory quality.

292 Principal Component Analysis (PCA) maps the natural, unsupervised conformation of samples'
293 groups and sub-groups [40]. **Figure 3A** shows the scores plot on the first two principal
294 components (F1-F2 plane), based on the 48 × 119 matrix (samples × targets). The variance
295 from the first principal component (F1) was 30.64% while for the second principal component
296 (F2) was 10.06%. Autoscaling and mean centering were applied as pre-processing methods,
297 because baseline correction already was applied for 2D data elaboration by GC Image. The
298 corresponding loading plots are available as Supplementary information (**Supplementary**
299 **Figure SF2A**).

300

301 **Insert here Figures 3A-B**

302

303 The PCA shows a clear discrimination between EVOO and VOO (clustered together in the right
304 side) and LOO samples. Additionally, a further sub-classification according to harvesting stage
305 is evident along F2 and within EVOO samples (see arrow).

306 The samples' structure/classification over the PCA loading plot (see Supplementary
307 Information **SF2A**) indicates those analytes that are effectively responsible for the
308 discrimination of *lampante* oils (stage 4 of *Benamaurel* and *Baza*). These analytes include
309 saturated (e.g., heptanal, octanal, and nonanal) and unsaturated (e.g., (*E*)-2-heptenal)
310 aldehydes, well-known from the literature to be correlated with specific sensory defects of
311 olive oils. Moreover, the separation of *lampante* oils is also driven by other compounds,
312 including some alcohols (e.g., propan-1-ol, 1-octen-3-ol, heptan-1-ol, and octan-1-ol), ketones
313 (e.g., heptan-2-one and octan-2-one) and esters (e.g., ethyl acetate, ethyl-2-methyl butanoate,
314 and ethyl-3-methyl butanoate).

1
2
3
4
5
6
7
8
9
10
11
12
13
14
15
16
17
18
19
20
21
22
23
24
25
26
27
28
29
30
31
32
33
34
35
36
37
38
39
40
41
42
43
44
45
46
47
48
49
50
51
52
53
54
55
56
57
58
59
60
61
62
63
64
65

315 Additional insight on the targets' distribution as a function of harvest time was obtained by
316 independently processing single subsets of samples by geographical location. In this way, all
317 variables related to the pedoclimatic conditions and field treatments (organic or conventional)
318 were excluded, and indications on variables (markers) correlated with ripening stage are more
319 clearly evidenced. **Figure 3B** shows the score plot for the *Caniles* EVOO subset and the
320 corresponding loadings plot is provided as Supplementary information (**Supplementary Figure**
321 **2B -SF2B**).

322 Compounds that contribute most to discriminating harvest stage 1 are: (Z)-2-hexenal,
323 connoted by a *fruity* note; (Z)-3-hexenal, with *green* odor; and (E,E)-2,4-hexadienal,
324 contributing a *fresh* note to the overall perception. A group of unsaturated hydrocarbons,
325 tentatively identified from the literature [41], was found to be distinctive in the discrimination
326 of the earlier harvest stages (1-2): 3,4-diethyl-1,5-hexadiene (RS+SR), 3,4-diethyl-1,5-
327 hexadiene (meso), (5Z)-3-Ethyl-1,5-octadiene, (5E)-3-Ethyl-1,5-octadiene, (E,Z)-3,7-decadiene,
328 (E,E)-3,7-decadiene, and (E)-4,8-Dimethyl-1,3,7-nonatriene. As expected, all these markers
329 decrease in later ripening stages.

330 Interestingly, but not surprisingly, the evolution of (Z)-2-hexenal and (Z)-3-hexenal, which
331 provide a *fruity* note (Mf), through time is in accordance with the sensory evaluation of the
332 panel (as reported in **Table 1**). The relative abundance of these analytes shows a marked
333 decrease from samples harvested in November (2014) to late January (2015). This observation
334 is confirmed by data from *Baza* oils where (Z)-3-hexenal falls below method Limit of Detection
335 (LOD) at stages 3 and 4 consistent with the perception of defects (Md>0.00) leading to their
336 classification as *lampante* oils, while (Z)-2-hexenal in *Benamaurel* samples was not detected
337 even at first harvesting time.

338 On the other hand, some other target analytes, for example octane (*sweetly, alcane*), nonanal
339 (*fatty, waxy*), and 6-methyl-5-hepten-2-one (*pungent, green*), showed an opposite trend by
340 increasing their relative abundance from stage 1 to the 4. Their presence was not revealed by
341 the panel, possibly because of their relatively high odor thresholds (octane 940 µg/Kg, nonanal
342 150 µg/Kg, and 6-methyl-5-hepten-2-one 1000 µg/Kg [22]).

343 These results are consistent with those reported by Aparicio and Morales [19], Raffo et al. [42]
344 and other researchers [22,43] who hypothesized an increase of autoxidation products (e.g.,
345 octane and 6-methyl-5-hepten-2-one) accompanied by a decrease of lipoxygenase pathway
346 products (e.g., (Z)-2-hexenal, (Z)-3-hexenal, and (E,E)-2,4-hexadienal) with later harvest times.
347 PCA carried out on *Baza* and *Benamaurel* oils (scores and loadings provided as Supplementary
348 information, **Supplementary Figures 3A and 3B - SF3A and SF3B**) confirms, with some

349 exceptions (e.g., in *Benamaurel* samples), the distribution of the samples and the trend of
350 these specific chemicals over time from stage 1 to 4.

351

352 3.2. Untargeted analysis

353 Untargeted analysis was performed to extend the comparative process to the entire
354 pattern of detected VOCs. The unsupervised fingerprinting was based on the peak-region
355 feature approach and implemented by Image Investigator in the GC Image software package.
356 This data elaboration step was made more informative by considering the 2D peaks included in
357 the targeted template built within the Step 1 of the work-flow (illustrated in **Figure 1**), thus
358 preserving all information about known analytes within the fingerprinting.

359 The fully automated procedure of *peak-regions* fingerprinting delineates a small 2D retention-
360 times window (or *region*) per 2D *peak* over the chromatographic space. Regions are shown in
361 **Figures 2B** and **2D**, delineated with light blue graphics. In this context, the process approaches
362 “one-feature-to-one-analyte” selectivity, typical of peak features methods, with all the
363 advantages of regional features matching [5,27,28]. These advantages includes unambiguous
364 cross-detection/matching of trace peaks that may be detected in some samples but not in
365 others and co-eluting analytes that may be resolved in some chromatograms but not in others.

366 The unsupervised procedure is:

- 367 1. Detect and record 2D peaks in individual chromatograms.
- 368 2. Locate *registration* peaks, i.e., peaks that reliably match across all chromatograms
369 (connoted by red circles in **Figures 2D** and **2E**). This is verified for a sub-group of
370 targeted peaks.
- 371 3. Align and combine all chromatograms to create a composite chromatogram [5].
- 372 4. Define a pattern of *region* features around every 2D peak detected in the composite
373 chromatogram.
- 374 5. Create a combined targeted and untargeted template from:
 - 375 a. the registration peaks from Step 2,
 - 376 b. the peak-regions from Step 4, and
 - 377 c. the targeted peaks.

378 The programmed output of the Image Investigator is the template that includes only (a) and
379 (b). An innovation of this work is the addition of (c) targeted peaks.

380 Once the resulting template, as shown in **Figure 2B** superimposed on the image of the *Baz_4_1*
381 sample - analytical replicate 1, is matched to a target chromatogram, the analysis includes
382 peak-regions (light blue graphics), targeted peaks (green circles), and registration peaks (red
383 circles). Feature regions are aligned relative to corresponding peaks, and the characteristics of

384 those features including all metadata (retention times in both chromatographic dimensions,
385 detector response, relative/absolute intensity, peaks' EI-MS fragmentation pattern, response
386 factors, etc.) are computed to create a feature vector for the target chromatogram to be
387 adopted for cross-sample analysis. The final output is a data matrix where peak-regions and
388 template peaks are cross-aligned within all samples' chromatograms and the response data
389 are available for further chemometrics.

390 Results based on 180 reliable peak-regions (i.e., those that matched in all-but-one
391 chromatogram of the set) are shown in **Figure 2B**, and visualized by PCA of **Figure 4A**. They
392 confirmed what already was evidenced by the known targets distribution: a clear
393 discrimination of *lampante* oils from VOO and EVOO while maintaining the sub-classification
394 based on harvesting period. These results account for a total variability of 42%, in line with
395 previous elaborations.

396 Targeted peak-regions cross-validate the classification based on PCA: (Z)-2-hexenal, (Z)-3-
397 hexenal, (E,E)-2,4-hexadienal, 1,4-pentadiene, (5Z)-3-ethyl-1,5-octadiene, and (E)-4,8-
398 dimethyl-1,3,7-nonatriene contribute to the discrimination of stages 1 and 2 against the
399 others, as obtained in the previous elaboration. Untargeted analysis does not discover
400 additional informative roles of un-identified features and confirms the coverage of the
401 targeted peaks.

402 One interesting and positive aspect of these results is the strong accordance between targeted
403 and untargeted fingerprinting in terms of sample discrimination effectiveness. This result was
404 not observed when, for example, sampling conditions included too many variables known to
405 impact the VOCs fingerprint (e.g., cultivars, geographical origin, harvesting period/year,
406 technological process, bad practices etc.) [8]. In those less-controlled cases, the sensitivity and
407 effectiveness of untargeted methodologies were lower and targeted analysis gave better
408 results. In such cases with more experimental variables, much larger numbers of samples may
409 be required for effective discrimination.

410 Another interesting outcome, in line with previous studies on flavor blueprint [8], is the
411 accordance between sensory quality scores and samples sub-classes. Because sensory profiles
412 by descriptive analysis were not available, a direct correlation between odor-active
413 compounds distribution and sensory quality was not possible. However, positive attributes (Mf
414 in **Table 1**) had high scores for samples harvested at stages 1 and 2 that rapidly decreased at
415 stages 3 to 4. Along the same Principal Component (e.g., F2) samples discrimination is in
416 accordance with both variables (i.e., quality score and ripening stage).

417 Cross-validation of fingerprinting results reinforces and confirms the role played by some
418 ripening markers responsible for positive attributes (green, fruity and fresh) [22,34]. These

419 compounds appear at stage 1, last up to the stage 2, and then start to decrease. From these
420 results, and in agreement with quality parameters (**Table 1**), the optimal harvest period to
421 obtain a product with high sensory quality from *Picual* variety appears to have been November
422 within stages 1 and 2.

423 Several informative analytes positively and/or negatively correlated with ripening and oil
424 quality, were therefore selected and their ratio profiled as a function of harvest stages. In
425 addition, a retrospective analysis on EVOO samples' pattern acquired during a previous study
426 [8] was performed to verify the reliability and consistency of these indicators.

427

428 *3.3 Retrospective analysis and definition of reliable chemical indexes of ripening*

429 Relative ratios (based on 2D Peak Volumes) from the informative chemicals highlighted by the
430 *UT fingerprinting* were calculated and trends observed along harvest stages.

431 These ratios are functions of sampling parameters (phase ratio, β ; sampling temperature; and
432 time), but derive from analyses conducted under highly standardized and head-space linearity
433 conditions. These VOCs fingerprints are therefore informative and replicable, and these ratios
434 could be transferred to other studies/ batches and considered as chemical indices of ripening.

435 Analytes chosen to discriminate samples at stages 1 and 2 were: (*Z*)-2-Hexenal, (*Z*)-3-Hexenal,
436 (*E*)-2-Pentenal, and (*E,E*)-2,4-Hexadienal; those chosen that contributed to discriminate the
437 late harvest stage were: octane, 6-methyl-5-hepten-2-one, and nonanal. Their ratios for the
438 *Baza* samples set are illustrated by the box-plot graphics in **Figure 5** and correspond to: (*Z*)-3-
439 Hexenal/6-Methyl-5-hepten-2-one, (*Z*)-3-Hexenal/Nonanal, (*Z*)-2-Hexenal/6-Methyl-5-hepten-
440 2-one, (*E,E*)-2,4-Hexadienal/6-Methyl-5-hepten-2-one, (*Z*)-3-Hexenal/Octane, (*E*)-2-
441 Pentenal/Nonanal, (*E*)-2-Pentenal/6-Methyl-5-hepten-2-one, and (*E*)-2-Pentenal/Octane.
442 Trends were estimated by fittings with exponential, polynomial, or linear functions to
443 delineate their evolution along harvest stage, resulting functions are reported in **Table 3**. The
444 accuracy of fittings is as assessed by the determination coefficient (R^2).

445

446 **Insert here Figure 5**

447

448 As a general consideration, most of the ratios followed an exponential or second order
449 polynomial trend with the exception of (*E*)-2-pentenal/octane index whose evolution was
450 relatively linear. In addition, non-linear trends are connoted by higher informative potential
451 because of their sudden changes between optimal and non-optimal ripening stages. Notably,
452 their numeric values decreased one order-of-magnitude between harvest stages where oil
453 quality changed from EVO to VO or *lampante*.

1 454 The usefulness of such ratios also might be evaluated from a wider perspective where, for
2 455 example, VOCs fingerprints are adopted for quality classification of EVO oils. Within selected
3 456 volatiles produced during the climacteric stage of ripening [22], (Z)-3-hexenal is a product of
4 457 the lipoxygenase pathway and, in EVO and VO oils, it contributes to the fresh aroma
5 458 perception thanks to its relatively low odor threshold [20,21,34,37]. This compound is also a
6 459 cultivar-specific marker for the *Picual* variety [34], as is 6-methyl-5-hepten-2-one that, as a
7 460 counterpart, is connoted by a negative odor perception and an incremental trend along
8 461 ripening stages. Nonanal provides information about oxidation state as well as octane
9 462 [36,37,44,45].

10 463 To evaluate the consistency and the transferability of this approach for informative chemical
11 464 indexes, a retrospective analysis was attempted by re-processing chromatograms from a
12 465 previous study [8]. Samples consisted of EVOO from different botanical/geographical origins
13 466 and technological processes and from olives harvested in 2013. They were analyzed previously,
14 467 in the authors' laboratory, with the same nominal HS-SPME sampling protocol and GC×GC-MS
15 468 conditions. Details are reported in **Table 1**.

16 469 The peak-regions template created in this study (and shown in **Figure 6A** with the *Can_1_2*
17 470 sample) was matched to these older, GC×GC chromatograms (as shown in **Figure 6B** with the
18 471 EVOO oil from Sicily PDO Monti Iblei) after a supervised transformation of the template to
19 472 compensate for non-linear retention times differences in both dimensions [46].

20 473

21 474 **Insert here Figures 6A-B**

22 475

23 476 These chromatographic inconsistencies are not infrequent because, in a time frame of two
24 477 years, column sets were replaced and/or columns have altered retention behaviour (in
25 478 particular the 1D PEG polar phase) producing minimal, but not negligible, pattern alterations.
26 479 However, thanks to the specificity of the matching methods, 2D peaks that positively match
27 480 are just those with EI-MS fragmentation pattern similarity above 700 (direct match) or 900
28 481 (reverse match). Cross-aligned results are in consequence reliable and consistent, making
29 482 possible retrospective investigations.

30 483 Ratios between informative markers for the EVOO samples from *Baza*, *Caniles*, and
31 484 *Benamaurel*, plus five samples from the previous study (R-EVOO from 1 to 5), were analyzed by
32 485 PCA and the results are shown in **Figure 4B**. The discrimination power of the first two PCs
33 486 reaches 94%, confirming the informative power of the combination of variables. *Picual*
34 487 samples (*Baz*, *Can* and *Ben*) are clustered together, with the exception of the *Benamaurel*
35 488 EVOO at the earliest harvest stage, whereas along F2, there is evident discrimination for

1
2
3
4
5
6
7
8
9
10
11
12
13
14
15
16
17
18
19
20
21
22
23
24
25
26
27
28
29
30
31
32
33
34
35
36
37
38
39
40
41
42
43
44
45
46
47
48
49
50
51
52
53
54
55
56
57
58
59
60
61
62
63
64
65

489 ripening stage. On the other hand, R-EVOO samples clustered together close to stages 2 and 3,
490 with the only exception of R-EVOO 2 PDO (Monti Iblei Sicily, Italy), which showed a very high
491 value for (Z)-3-Hexenal/6-Methyl-5-hepten-2-one because of the high abundance of (Z)-3-
492 Hexenal (which accounted for 12% of Total Volume). The corresponding loading plot for
493 informative ratios is provided as Supplementary information **Supplementary Figure 4B - SF4B**.
494 The proposed ratios are consistent within Picual variety, but to be considered as general
495 indices for ripening classification their reliability should be verified and validated by analyzing
496 samples from different harvest years and location, and their transferability to other botanical
497 origins and geographical locations should be investigated ex-novo by screening samples after a
498 rigorous sampling design.

500 *3.4 Fingerprinting by image features approach*

501 The last part of this study focuses on a fingerprinting approach based on *visual*
502 features and it is suitable for rapid and effective pair-wise pattern comparisons. The approach
503 is one of the earliest introduced in GC×GC data elaboration [5], and is still adopted when
504 distinctive patterns have to be compared on an untargeted basis to immediately reveal
505 compositional differences.

506 Previous studies demonstrated the potentials of this simple and intuitive approach by
507 exploring the volatile fraction of roasted coffee and juniper [47], volatiles emitted from
508 *Chrysolina herbacea* bugs fed by *Mentha* spp. leaves [48], and primary metabolites distribution
509 in mice urine after dietary manipulation [26]. The same approach was used iteratively, by cross
510 matching sample pairs, to reveal a chemical blueprint of odor active compounds responsible of
511 sensory defects [8].

512 In this application, where VOCs variations are mainly related to harvest/ripening stage, the
513 visual approach would be effective to immediately highlight 2D peaks and/or analytes that
514 have significantly different relative distributions between sample pairs. In addition, by
515 comparing samples within the same production plot, the effect of fruit maturation is magnified
516 while keeping constant the effect of local pedoclimatic changes.

517 This fully automated approach, namely Image Comparison (GC Image v2.5b), if implemented
518 with peak-regions fingerprinting template, provides immediate information about targeted or
519 untargeted peak-regions variations between pair-wise compared samples.

520 The example here illustrated refers to a *Benamaurel* oil sample obtained at stage 1 (averaged
521 normalized image from *Ben_1_1* and *Ben_1_2*) arbitrarily considered as the *analyzed* image
522 versus the stage 4 samples (averaged normalized image from *Ben_4_1* and *Ben_4_2*) arbitrarily
523 considered as the *reference* image.

524 **Figure 7** shows the image comparison results between the average image of harvest stage 1
525 (**Fig. 7A**) and stage 4 (**Fig. 7B**) obtained by averaging the 2D chromatograms from two replicate
526 locations and two analytical runs. The resulting image (**Fig. 7C**) is rendered as “colorized fuzzy
527 ratio” that uses the Hue-Intensity-Saturation (HIS) color space to color each pixel in the
528 retention-times plane. The algorithm computes the difference at each data point between
529 aligned pair-wise images. If a pixel is colored green, then the difference is positive, indicating a
530 larger detector response in the *analyzed* image (*Ben_1_1 and Ben_1_2*). If a pixel is colored
531 red, then the difference is negative, indicating a larger detector response in the *reference*
532 image (*Ben_4_1 and Ben_4_2*). Brightness depends on the magnitude of the difference, and
533 so white saturation indicates pixels at which peaks have detector responses that are nearly
534 equal in the analyzed and reference images.

535

536 **Insert here Figures 7A-C**

537

538 Because the 2D chromatograms submitted to the image comparison were already pre-
539 processed by *peak-region* fingerprinting, results are implemented with the information about
540 2D peaks’ identity (if known) or unique identification numbering (#) for unknowns.

541 Results of *visual* features fingerprinting are intuitive and promptly give information on
542 discriminant peaks. Green colored regions in the upper part of the 2D plot at lower ¹D
543 retention correspond to unsaturated alkanes [41] (#ID 10, 11, 15, 17, 21), unsaturated
544 aldehydes (#30 (E)-2-Pentenal, #32 (Z)-3-Hexenal, #34 (E)-3-Hexenal, #42 (Z)-2-Hexenal, #44 (E)-
545 2-Hexenal, #71 (E,Z)-2,4-Hexadienal, and #73 (E,E)-2,4-Hexadienal), whereas red areas
546 corresponds to limonene (#41), short chain fatty acids (#107 hexanoic, #115 octanoic and #117
547 nonanoic acid), linear saturated aldehydes (#12 pentanal, #54 octanal and #70 decanal), and
548 some ketones, such as 6-methyl-5-hepten-2-one (#63).

549

550 **4. Conclusions**

551 This study evidences and emphasizes the potentials of fingerprinting based on GC×GC-
552 MS separations and highlights the synergism between untargeted and targeted methodologies
553 to investigate complex fractions of volatiles in depth. Their combination enables to achieve the
554 most inclusive/comprehensive fingerprinting (*UT fingerprinting*) and if compared to previous
555 studies, the degree of automation implemented in the data elaboration work-flow is
556 promising. Experimental results on EVOO volatiles definitely confirm the maturity of available
557 software tools to exploit dense and multi-level data set effectively.

1
2
3
4
5
6
7
8
9
10
11
12
13
14
15
16
17
18
19
20
21
22
23
24
25
26
27
28
29
30
31
32
33
34
35
36
37
38
39
40
41
42
43
44
45
46
47
48
49
50
51
52
53
54
55
56
57
58
59
60
61
62
63
64
65

558 The consistency and reliability of cross-sample analysis results in revealing
559 informative/discriminant features is confirmed by matching results from different approaches,
560 and is of interest in this challenging application field where accurate fingerprinting can be very
561 useful: (a) to support studies aimed at improving product quality; (b) to define a distinctive
562 chemical fingerprint to discriminate samples of a certain botanical/geographical origin; and (c)
563 to re-investigate, on a retrospective projection, samples in light of new informative features.
564

1
2
3
4
5
6
7
8
9
10
11
12
13
14
15
16
17
18
19
20
21
22
23
24
25
26
27
28
29
30
31
32
33
34
35
36
37
38
39
40
41
42
43
44
45
46
47
48
49
50
51
52
53
54
55
56
57
58
59
60
61
62
63
64
65

565 **Acknowledgments**

566 The authors are grateful to “GDR Altiplano de Granada” (Spain) for olives samples.

567 The research was carried out thanks to the support "International mobility program for young
568 researchers (PhD)” by University of Granada and CEI BioTic Granada.

569

570 Note: S. E. Reichenbach has a financial interest in GC Image, LLC.

571

572 **Figure Captions:**

573 **Figure 1:** Two-dimensional chromatographic data elaboration work-flow.

574

575 **Figures 2A-E:** (2A) Pseudocolored GC×GC chromatogram of *Ben_4_1* harvested at stage 4 (in
576 January 2015). (2B) Position of the 119 known target peaks (empty light green circles) linked to
577 the ISTD (α -tujone black circle) by red lines. (2C) Retention area of highly volatile compounds
578 referred to the white rectangle of Fig. 2A. (2D) Peak-regions delineated by light blue graphics
579 together with targeted peaks (empty light blue circles). (2E) Results of comprehensive
580 template matching for peak-regions, target peaks (green circles) and registration peaks (red
581 circles). For details see text.

582

583 **Figures 3A-B:** PCA results. (3A) Scores plot on the first two principal components (F1-F2 plane),
584 based on targets distribution across all samples (48 × 119 matrix - samples × targets). (3B)
585 Scores plot the first two principal components (F1-F2 plane) based on targets distribution
586 across *Caniles* EVOO subset.

587

588 **Figures 4A-B:** PCA results. (4A) Scores plot on the first two principal components (F1-F2 plane),
589 based on reliable *peak-regions* distribution across all samples (48 × 180 matrix - samples ×
590 reliable *peak-regions*). (3B) Scores plot the first two principal components (F1-F2 plane) based
591 on informative ratios between ripening markers. For details see text.

592

593 **Figure 5:** Box-plot graphics showing the evolution of different informative ratios between
594 ripening markers along harvest stages for Baza plot samples.

595

596 **Figures 6A-B:** (6A) 2D chromatogram of *Can_1_2* sample together with the reliable peak-
597 regions template. (6B) 2D chromatogram of *R-EVOO 2* sample (PDO Monti Iblei - Sicily Italy)
598 together with the reliable peak-regions template tranformed and adapted with a supervised
599 approach.

600

601 **Figures 7A-C:** (7A) Averaged 2D-chromatogram of *Benamaurel* oil samples (field replicates and
602 analytical replicates) obtained at stage 1 and (7B) at stage 4. (7C) Image comparison results
603 between average image of harvest stage 1 (7A) and stage 4 (7B). The resulting image is
604 rendered as “colorized fuzzy ratio”. Analytes that varied between stages are listed together
605 with their unique ID numbering (ref. Table 2).

606

1
2
3
4
5
6
7
8
9
10
11
12
13
14
15
16
17
18
19
20
21
22
23
24
25
26
27
28
29
30
31
32
33
34
35
36
37
38
39
40
41
42
43
44
45
46
47
48
49
50
51
52
53
54
55
56
57
58
59
60
61
62
63
64
65

607 **Table Captions:**

608

609 **Table 1:** List of analyzed samples together with plot denomination, field replicate, harvest
610 stage, acronym, quality parameters according to COMMISSION REGULATION (EEC) No 2568/91
611 of 11 July 1991, sensory evaluation results, and commercial classification.

612

613 **Table 2:** List of the 119 target analytes together with ¹D and ²D retention times, I_s^T and sensory
614 descriptors as reported in reference literature [31,32,33,34,35,36,37,38,39]. The 2D Peak
615 Volume data is provided as Supplementary information in **Supplementary Table 1 - ST1**.

616

617 **Table 3:** Ripening informative markers evolution trends along harvest stages. The quality of
618 fittings is referred as Coefficient of Determination (R^2).

619

- [1] P.Q. Tranchida, P. Donato, F. Cacciola, M. Beccaria, P. Dugo, L. Mondello, Potential of comprehensive chromatography in food analysis. *TrAC Trends Anal Chem* 52 (2013) 186-205
- [2] C. Cordero, J. Kiefl, P. Schieberle, S.E. Reichenbach, C. Bicchi, Comprehensive two-dimensional gas chromatography and food sensory properties: potential and challenges. *Anal. Bioanal. Chem.* 407 (2015) 169-191.
- [3] C. Giddings, Sample dimensionality: a predictor of order-disorder in component peak distribution in multidimensional separation, *J. Chromatogr. A* 703 (1995) 3-15
- [4] Z. Zeng, J. Li, H.M. Hugel, G. Xu, P.J. Marriott, Interpretation of comprehensive two-dimensional gas chromatography data using advanced chemometrics. *TrAC Trends Anal Chem* 53 (2014) 150-66
- [5] S.E. Reichenbach, X. Tian, C. Cordero, Q. Tao, Features for non-targeted cross-sample analysis with comprehensive two-dimensional chromatography, *J. Chromatogr. A* 1226 (2012) 140-148
- [6] S.E. Reichenbach, P.W. Carr, D.R. Stoll, Q. Tao, Smart templates for peak pattern matching with comprehensive two-dimensional liquid chromatography. *J. Chromatogr. A* 1216 (2009). 3458-3466.
- [7] P.Q. Tranchida, G. Purcaro, M. Maimone, L. Mondello, Impact of comprehensive two-dimensional gas chromatography with mass spectrometry on food analysis. *J Sep Sci* 39 (2016) 149-61
- [8] G. Purcaro, C. Cordero, E. Liberto, C. Bicchi, L. S. Conte, Toward a definition of blueprint of virgin olive oil by comprehensive two-dimensional gas chromatography. *J. Chromatogr. A*, 1334 (2015) 101-111.
- [9] L.T. Vaz-Freire, M.D.R.G. da Silva, A.M.C. Freitas, Comprehensive two-dimensional gas chromatography for fingerprint pattern recognition in olive oils produced by two different techniques in portuguese olive varieties galega vulgar, cobrançosa e carrasquenha. *Anal Chim Acta* 633 (2009) 263-70.
- [10] T. Cajka, K. Riddellova, E. Klimankova, M. Cerna, F. Pudil, J. Hajslova, Traceability of olive oil based on volatiles pattern and multivariate analysis. *Food Chem* 121 (2010) 282-9
- [11] C. Cordero, E. Liberto, C. Bicchi, P. Rubiolo, S.E. Reichenbach, X. Tian, Q. Tao, Targeted and non-targeted approaches for complex natural sample profiling by GC×GC -qMS. *J Chromatogr Sci* 48 (2010) 251-61.
- [12] C. Cordero, E. Liberto, C. Bicchi, P. Rubiolo, P. Schieberle, S.E. Reichenbach, Q. Tao, Profiling food volatiles by comprehensive two-dimensional gas chromatography coupled with mass spectrometry: Advanced fingerprinting approaches for comparative analysis of the volatile fraction of roasted hazelnuts (*Corylus avellana* L.) from different origins. *J Chromatogr A* 1217 (2010) 5848-58.
- [13] M.N. Franco, J. Sánchez, C. De Miguel, M. Martínez, D. Martín-Vertedor. Influence of the fruit's ripeness on virgin olive oil quality. *J. Oleo Sci.*, 64 (3) (2015), 263-273.
- [14] L.C. Matos, S.C. Cunha, J.S. Amaral, J.A. Pereira, P.B. Andrade, R.M. Seabra, B.P.P. Oliveira, Chemometric characterization of three varietal olive oils (Cvs. Cobrançosa, Madural and Verdeal Transmontana) extracted from olives with different maturation indices. *Food Chem.*, 102 (2007). 406-414.
- [15] L. Martínez Nieto, G. Hodaifa, J.L. Lozano Peña, Changes in phenolic compounds and rancimat stability of olive oils from varieties of olives at stages of ripeness. *J Sci Food Agric.* 90, (2010) 2393-2398.
- [16] T.Gallina-Toschi, L. Cerretani, A. Bendini, M. Bonoli-Carbognin, G. Lercker, Oxidative stability and phenolic content of virgin olive oil: an analytical approach by traditional and high resolution techniques. *J. Sep. Sci.* 28 (2005). 859-870.

-
- 1 [17] L. Nasini, P. Proietti, Olive harvesting. In: Peri C. (ed). The extra-virgin olive oil handbook.
2 John Wiley Blackwell, Chichester (UK) (2014). pp. 89-105.
- 3 [18] M.N. Franco, J. Sánchez, C. De Miguel, M. Martínez, D. Martín-Vertedor, Influence of the
4 fruit's ripeness on virgin olive oil quality. *J. Oleo Sci.*, 64 (3) (2015). 263-273.
- 5 [19] R. Aparicio, M.T. Morales, Characterization of olive ripeness by green aroma compounds
6 of virgin olive oil. *J Agric Food Chem*, 46 (1998) 1116-1122.
- 7 [20] Morales M.T., Aparicio R., Calvente J.J.. Influence of olive ripeness on the concentration of
8 green aroma compounds in virgin olive oil. *Flav. Frag. J.*, 11 (1996) 171-178.
- 9 [21] R. Aparicio, G. Luna, Characterisation of monovarietal virgin olive oils. *Eur. J. Lipid Sci.*
10 *Technol.* 104, (2002). 614-627.
- 11 [22] C.M. Kalua, M.S. Allen, Jr. Bedgood, A.G. Bishop, P.D. Prenzler, K. Robards, Olive oil volatile
12 compounds, flavour development and quality: A critical review. *Food. Chem.* 100 (2007) 273-
13 286.
- 14 [23] A.M. Inarejos-García, M. Santacatterina, M.D. Salvador, G. Fregapane, S. Gómez-Alonso,
15 PDO virgin olive oil quality-Minor components and organoleptic evaluation. *Food Res. Int.* 43
16 (2010). 2138-2146.
- 17 [24] Regulation EU No 1348/2013 on the characteristics of olive oil and olive-residue oil and on
18 the relevant methods of analysis
- 19 [25] S.E. Reichenbach, D.W. Rempe, Q. Tao, D. Bressanello, E. Liberto, C. Bicchi, S. Balducci, C.
20 Cordero, Alignment for comprehensive two-dimensional gas chromatography with dual
21 secondary columns and detectors. *Anal Chem* ;87(19) (2015) 10056-63
- 22 [26] D. Bressanello, E. Liberto, M. Collino, S.E. Reichenbach, E. Benetti, F. Chiazza, C. Bicchi, C.
23 Cordero, Urinary metabolic fingerprinting of mice with diet-induced metabolic derangements
24 by parallel dual secondary column-dual detection two-dimensional comprehensive gas
25 chromatography. *J Chromatogr A* ;1361 (2014) 265-76.
- 26 [27] S.E. Reichenbach, X. Tian, A.A. Boateng, C.A. Mullen, C. Cordero, Q. Tao, Reliable peak
27 selection for multisample analysis with comprehensive two-dimensional chromatography. *Anal*
28 *Chem* 85(10) (2013)4974-81.
- 29 [28] S.E. Reichenbach, X. Tian, Q. Tao, E.B. Ledford, Jr., Z. Wu, O. Fiehn. Informatics for cross-
30 sample analysis with comprehensive two-dimensional gas chromatography and high-resolution
31 mass spectrometry (GCxGC-HRMS). *Talanta* 83(4) (2011) 1279-88.
- 32 [29] B. Hollingsworth, S. Reichenbach, Q. Tao, and A. Visvanathan. "Comparative Visualization
33 for Comprehensive Two-Dimensional Gas Chromatography." *Journal of Chromatography A*,
34 1105(1-2):51-58, 2006
- 35 [30] COMMISSION REGULATION (EEC) No 2568/91 of 11 July 1991 on the characteristics of
36 olive oil and olive-residue oil and on the relevant methods of analysis and successive
37 emendments.
- 38 [31] K. Kotsiou, M. Tasioula-Margari, Changes occurring in the volatile composition of Greek
39 virgin olive oils during storage: oil variety influences stability. *Eur. J. Lipid Sci. Technol.* 117
40 (2015). 514-522.
- 41 [32] I. Romero, D. L. García-González, R. Aparicio-Ruiz, M. T. Morales, Validation of SPME-
42 GCMS method for the analysis of virgin olive oils volatiles responsible for sensory defects.
43 *Talanta*, 134 (2015) 394-401.
- 44 [33] L. Cerretani, M. Desamparados Salvador, A. Bendini, G. Fregapane, Relationship between
45 sensory evaluation performed by Italian and Spanish official panels and volatile and phenolic
46 profiles of virgin olive oils. *Chem. Percept.* 1 (2008) 258-267.
- 47 [34] G. Luna, M. T. Morales, R. Aparicio, Characterisation of 39 varietal virgin olive oils by their
48 volatile composition. *Food Chem.*, 98 (2006) 243-252.
- 49 [35] R. Iraqi, C. Vermeulen, A. Benzekri, A. Bouseta, S. Collin, Screening for key odorants in
50 Moroccan green olives by gas chromatography-olfatometry/aroma extract dilution analysis. *J.*
51 *Agric. Food Chem.*, 53 (2005) 1179-1184.
- 52
53
54
55
56
57
58
59
60
61
62
63
64
65

-
- 1 [36] M. T.Morales, G. Luna, R. Aparicio, Comparative study of virgin olive oil sensory defects.
2 Food Chem., 91 (2005) 293-301.
- 3 [37] Reiniers J., Grosch W. Odorants of virgin olive oils with different flavor profiles. J. Agric.
4 Food Chem. 46 (1998) 2754-2763.
- 5 [38] M. Rychlik, P. Schieberle, W. Grosch (1998). Compilation of odor thersholds, odor qualities
6 and retention indeces of key food odorants. Deutsche Forschungsanstalt für
7 Lebensmittelchemie and Institut für Lebensmittelchemie der Technischen Universität
8 München. Garching, Germany.
- 9 [39] <http://www.flavornet.org/flavornet.html> [Check: 02 May 2016].
- 10 [40] R. Leardi (2003). Chemometrics in data analysis. In: Lees M. (ed). Food authenticity and
11 traceability. Ed. Woodhead, Cambridge.
- 12 [41] F. Angerosa, L. Camera, N. D'Alessandro, G. Mellerio Characterization of seven new
13 hydrocarbon compounds present in the aroma of virgin olive oils, J. Agric. Fodd Chem. 46 (2)
14 (1998) 648-653
- 15 [42] A. Raffo, R. Bucci, A. D'Aloise, G. Pastore Combined effects of reduced malaxation oxygen
16 levels and storage time on extra-virgin olive oil volatiles investigated by a novel chemometric
17 approach. Food Chem. 182 (2015) 257-267.
- 18 [43] M.D.R.Gomes da Silva, A.M. Costa Freitas, M.J.B. Cabrita, Garcia Raquel. Olive oil
19 composition: volatile compounds, in: Boskou D. Olive oil-constituents, quality, health
20 properties and bioconversions, Rijeka, Croatia, 2011, pp. 17-46.
- 21 [44] V.Messina, A. Sancho, N. Walsöe de Reca Monitoring odour of heated extra-virgin olive
22 oils from Arbequina and Manzanilla cultivars using an electronic nose. Eur. J. Lipid Sci.
23 Technol. 117 (2015) 1-6.
- 24 [45] A. Kanavouras, P. Hernandez-Münoz, F. Coutelieris, S. Selke Oxidation-derived flavor
25 compounds as quality indicators for packaged olive oil. J. Am. Oil Chem. Soc., 81, (2004) 251-
26 257.
- 27 [46] GC Image, LLC. GC Image GCxGC Edition Users' Guide, R2.6, 2016
- 28 [47] C. Cordero, E. Liberto, C. Bicchi, P. Rubiolo, S.E. Reichenbach, X. Tian, Q. Tao. Targeted and
29 non-targeted approaches for complex natural sample profiling by GCxGC-qMS. J. Chromatogr.
30 Sci. 48 (2010) 251.
- 31 [48] C. Cordero, S.A. Zebelo, G. Gnavi, A. Griglione, C. Bicchi, M.E. Maffei, P. Rubiolo, HS-
32 SPME-GCxGC-qMS volatile metabolite profiling of Chrysolina herbacea frass and Mentha spp.
33 leaves. Analytical and Bioanalytical Chemistry 402 (2012) 1941-1952
- 34
35
36
37
38
39
40
41
42
43
44
45
46
47
48
49
50
51
52
53
54
55
56
57
58
59
60
61
62
63
64
65

Figure 1

[Click here to download Figure: Figure 1.pptx](#)

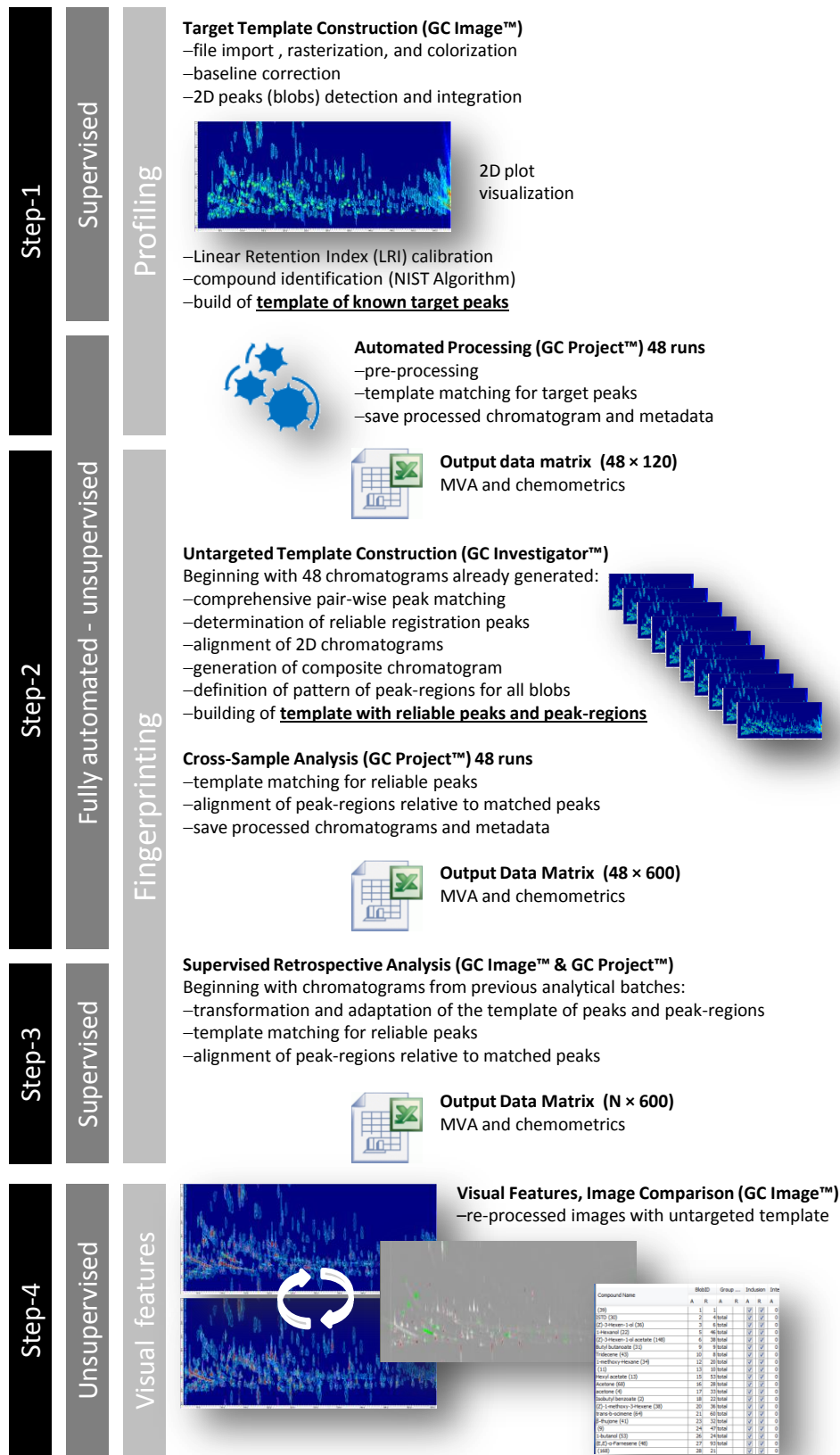


Figure 2 new
Click here to download Figure: Figure 2rev.pptx

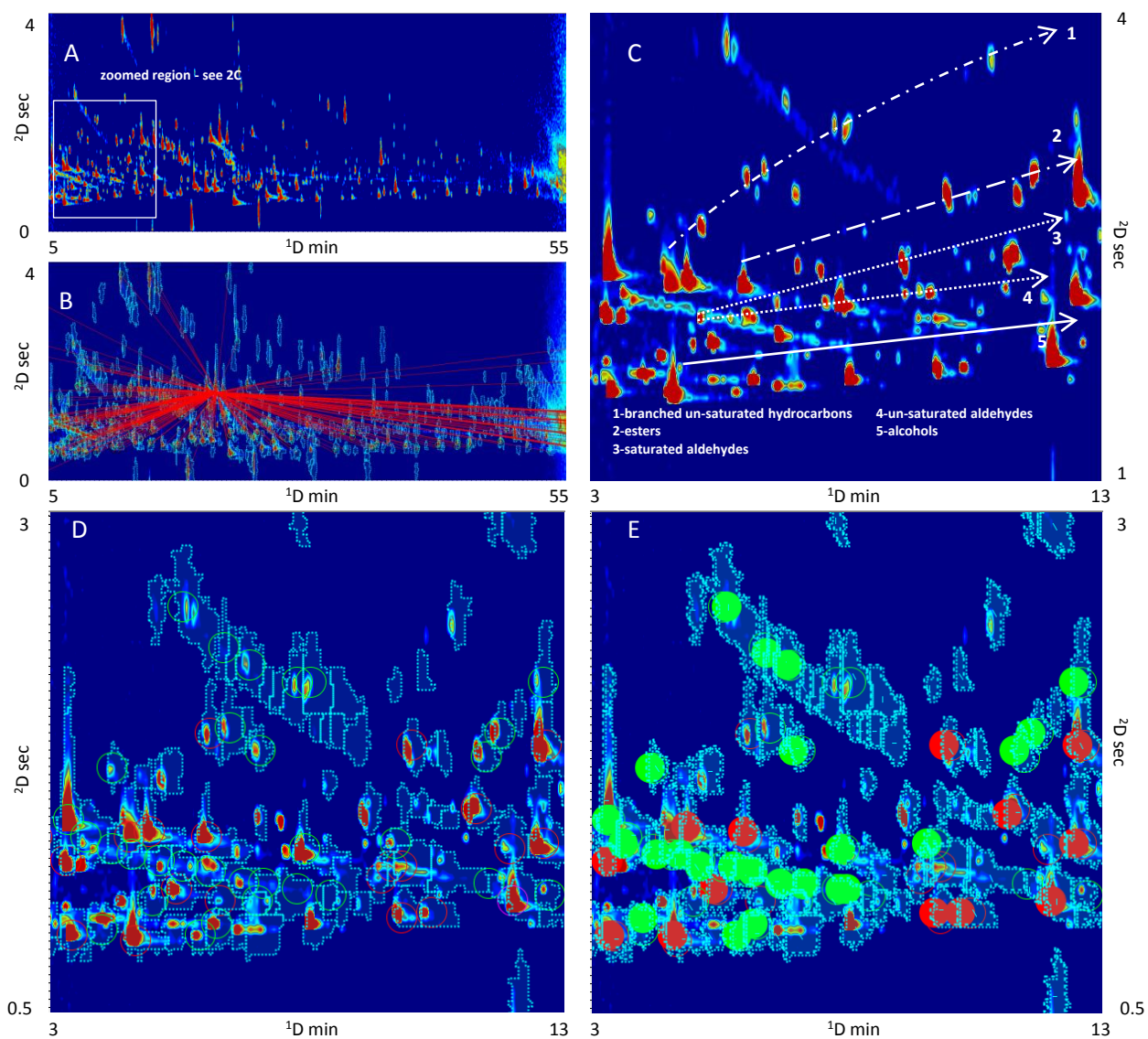


Figure 3

[Click here to download Figure: Figure 3.pptx](#)

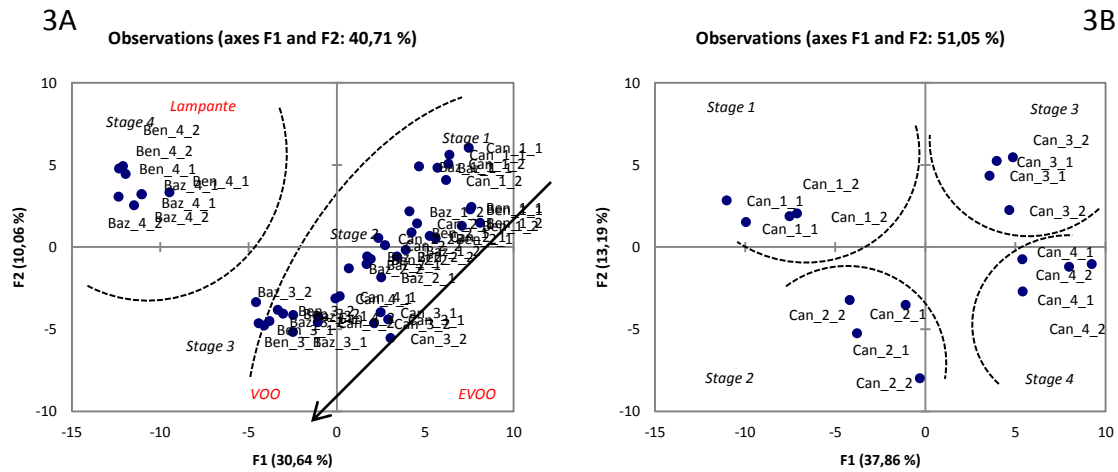


Figure 4

[Click here to download Figure: Figure 4.pptx](#)

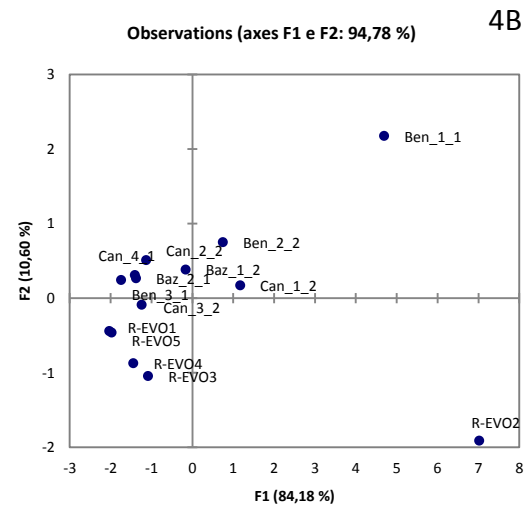
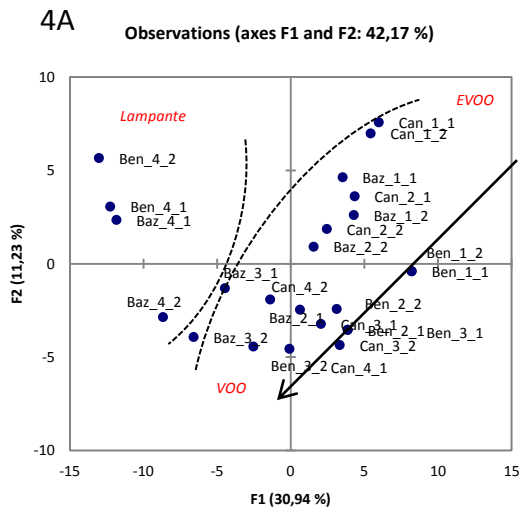


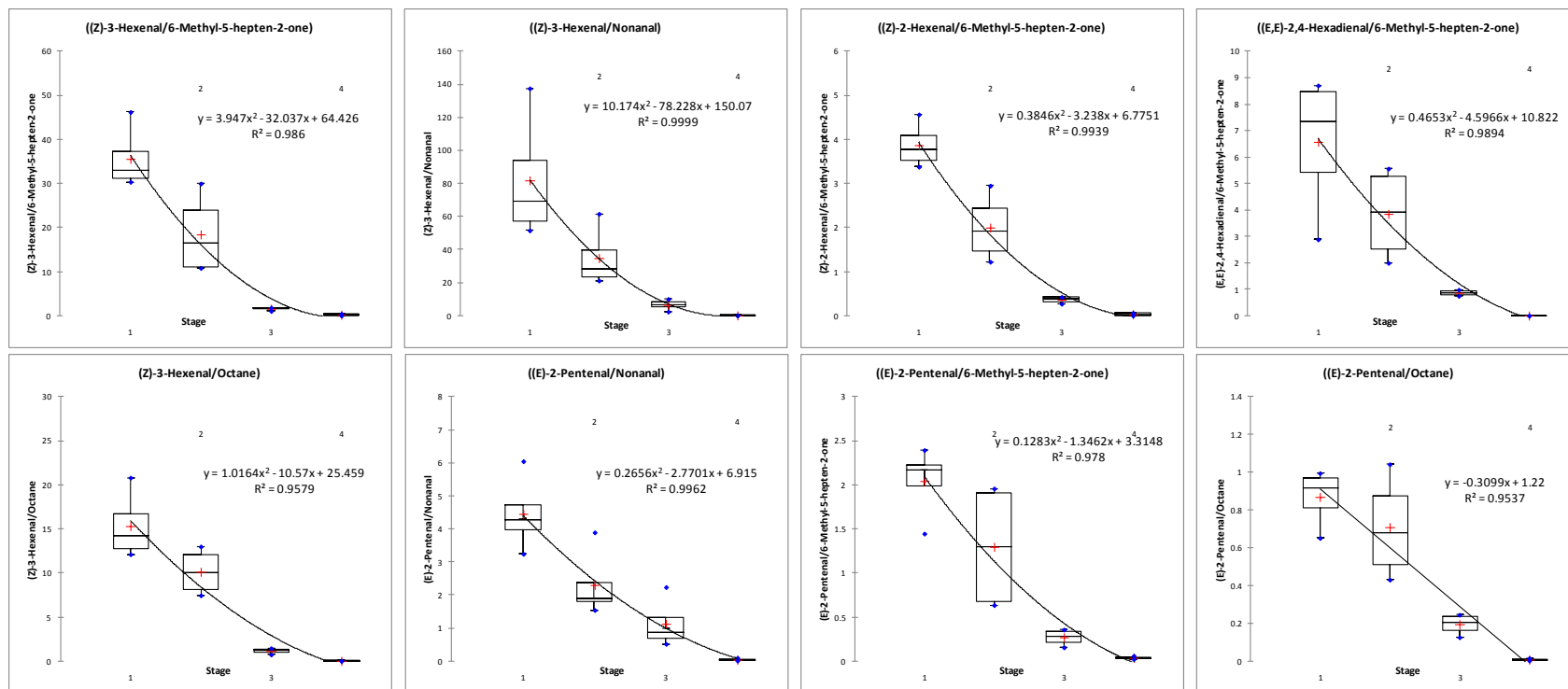
Figure 5[Click here to download Figure: Figure 5.pptx](#)

Figure 6
[Click here to download Figure: Figure 6.pptx](#)

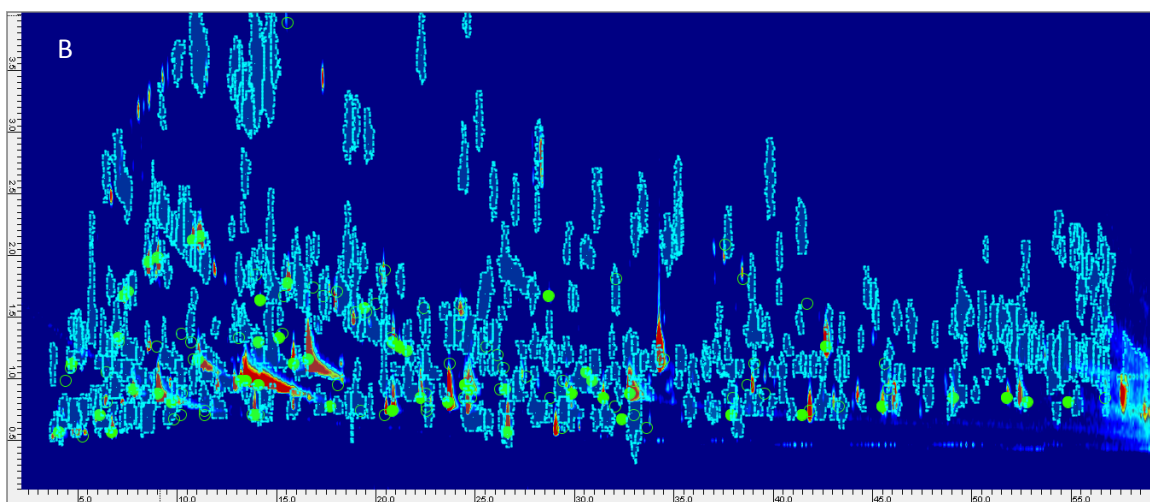
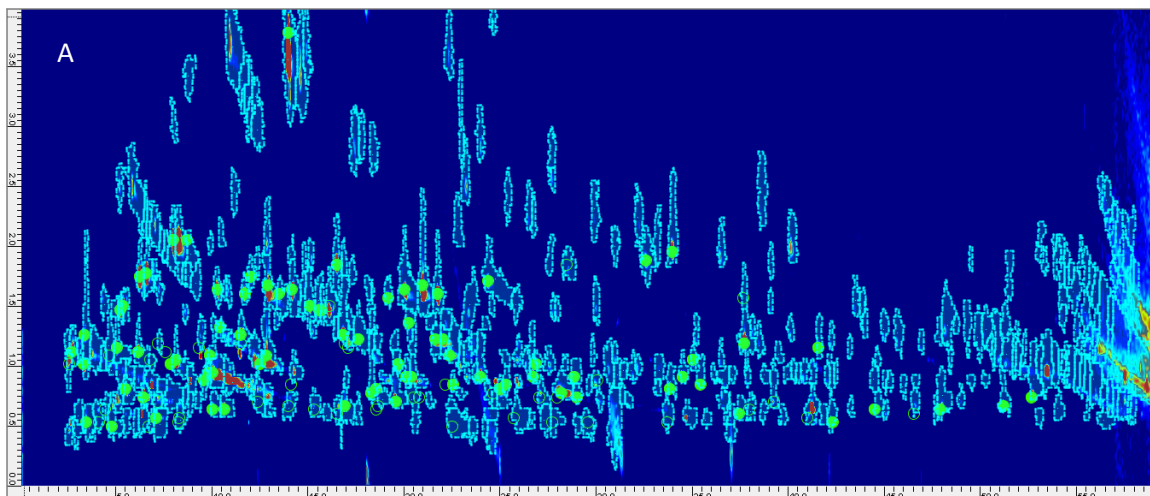
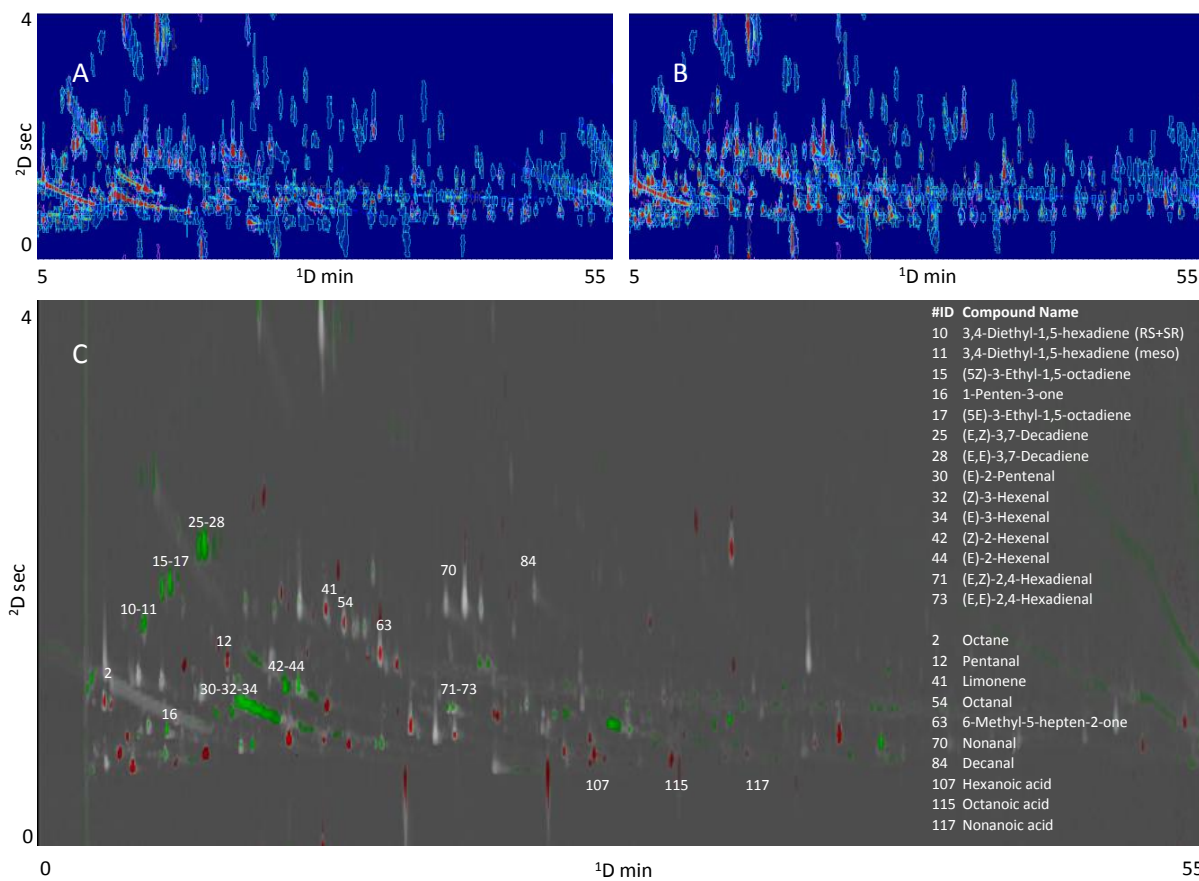


Figure 7 new

[Click here to download Figure: Figure 7rev.pptx](#)



Electronic Supplementary Material (online publication only)

[Click here to download Electronic Supplementary Material \(online publication only\): Supplementary Table 1.xlsx](#)

Electronic Supplementary Material (online publication only)

[Click here to download Electronic Supplementary Material \(online publication only\): Supplementary Table 2.xlsx](#)

Electronic Supplementary Material (online publication only)

[Click here to download Electronic Supplementary Material \(online publication only\): Supplementary Information.pptx](#)